A Novel Algorithm for Extraction of the Layers of the Cornea

J.A. Eichel, A.K. Mishra, D.A. Clausi, P.W. Fieguth, K.K. Bizheva
jaeichel, akmishra, dclausi, pfieguth, kbizheva@uwaterloo.ca
Vision and Image Processing Group, University of Waterloo, Canada

Abstract

Accurate corneal layer boundary extraction from optical coherence tomography can provide precise layer thickness measurements required in the analysis of corneal disease. This paper establishes a novel approach to precisely obtain the five primary corneal layer boundaries. The proposed method determines correspondence relationships between the layer boundaries to facilitate robust boundary extraction in the presence of noise and artifacts. The first phase of the method applies morphological operators to enhance the prominent structural features of the cornea. The second phase uses a semi-automated segmentation algorithm to extract the upper and lower boundaries of the cornea; these boundaries are used to register the corneal image. The final phase extracts all five boundaries using a global optimization method exploiting the medial correspondence relationship between each layers.

The proposed method is tested and verified using a representative set of optical coherence tomography images and compared against several state of the art methods. The proposed method is demonstrated to be more robust to noise, to provide more accurate segmentation results, and to require fewer user interactions than the other published methods.

1. Introduction

The adult cornea is only about 1/2 millimeter thick and is comprised of five layers: epithelium, Bowman's membrane, stroma, Descemet's membrane and the endothelium [1, 8]. The precise measurement of the thickness of all cornea layers is essential for the analysis of corneal swelling, acidosis, and altered corneal oxygen consumption [9]. To obtain corneal images, optical coherence tomography (OCT) technology is used to capture the internal structure of the cornea. The images produced using OCT are characterized by low signal to noise ratio and image non-homogeneities. Robust and accurate boundary extraction poses a great challenge.

Kostadinka et al. [14] first captured the cornea layers using a high speed, ultra high refractive optical coherence tomography (UHROCT) imaging technology and then applied image processing algorithms, such as Fuzzy Type II wavelet despeckling. Although the images have been captured and denoised, there is no computer vision literature related to corneal layer boundary extraction to obtain the precise measurement of layer thickness.

However, existing methods such as active contour [2, 4, 7, 10], intelligent scissors [5], enhanced intelligent scissor [12], and edge relaxation and linking techniques could be adapted for segmentation of the layers of the cornea. Active contours or deformable models, fully-automatic segmentation approaches, are typically used to extract the layer boundaries. Unfortunately, none of these approaches are suitable for corneal layer extraction because the layers of the cornea are characterized by low signal to ratio. Consequently, these fully-automated segmentation methods are not capable of extracting layer boundaries. Rather, rigid model based approaches are preferred.

Mortenson et al. [5] first introduced intelligent scissors (IS), a semi-automatic segmentation algorithm, which assists the user during the interactive segmentation process. The user interaction allows the process to take advantage of user knowledge when defining the boundaries. For this method, the user selects seed points on the boundary and, as the mouse moves along the boundary, the optimal boundary path between the starting point and the current point is obtained. There are two main advantages to this approach to segmentation. First, the segmentation is accomplished in real-time; this allows for rapid image segmentation. Second, the boundary accuracy resulting from this type of method is generally higher than automatic methods since user knowledge is utilized throughout the process [5].

However, there are several drawbacks to existing IS-based methods for precise measurement of cornea thickness. First, like current automatic segmentation methods, the boundary definition for existing IS methods rely on image gradients; this dependence makes the algorithm sensitive to contrast non-uniformities found in low signal to noise ratios associated with OCT cornea images. Second, existing IS methods require the clinician to perform relatively accurate manual tracing along the region boundary, which

can be time-consuming and laborious, particularly for complex regions of interest. To overcome some of the problems associated with IS, Wong et al. [12] proposed enhanced intelligent scissors (EIS) that uses phase-based representation of the image as the external local cost, instead of the image gradient. However, EIS approach alone is not suitable for the extraction of the layers of the cornea.

To precisely locate the layers of the cornea, this paper proposes a semi-automatic model based segmentation method designed to minimize user input. First, the algorithm identifies the epithelium (upper) and the endothelium (lower) layer of the cornea using enhanced intelligent scissor (EIS), a user-interactive semi-supervised segmentation method. Second, a correspondence model is established between the upper and lower layer of the cornea using medial axis transform (MAT). Finally, the boundaries are determined from discrete optimization followed by parameter estimation using prior information, the correspondence between layers extracted using medial axis transform relationship.

The proposed method is described in Section 3. Section 4 demonstrates the use of proposed method to extract the layers of the cornea. Finally, the conclusion and future research are discussed in Section 5.

2 Theory of the Proposed Method

The OCT corneal image contains five distinct layer boundaries and is illustrated in figure 2. The epithelium and endothelium outer boundaries have the highest contrast and the Descemet's membrane has the lowest contrast.

Several corneal images are initially segmented using the following methods: a edge linking and relaxation labeling [6], parametric active contours [7, 4], geometric active contours [10], optimal boundary detection [11] and edge-free active contours [3] to extract the five layers of the cornea. Unfortunately, none of these method give satisfactory segmentation results for the corneal image. The failure of these methods are due to following reasons:

- The OCT image has low signal to noise ratio and contains image non-homogeneities.
- The boundary detection methods are dependent upon the image gradient obtained from the noisy OCT image.
- The inner boundaries of the OCT image are indistinct.

The poor performance of the geometric active contour, one of the better segmentation algorithms, is illustrated in figure 1.

Instead, a model of the cornea is used to guide active contours to segment the noisy image. Let the layer boundaries be represented using continuous parametric curves.

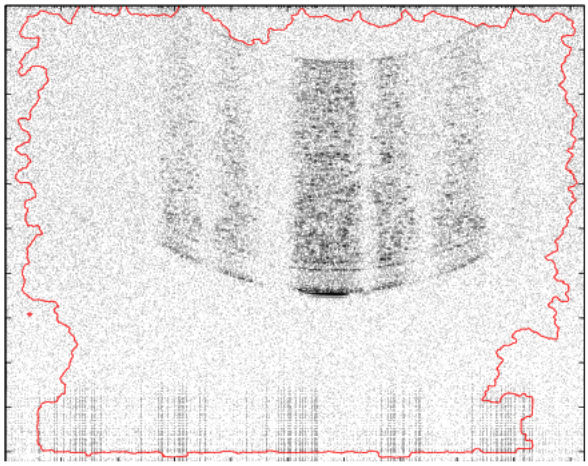

Figure 1. The level set based geometric active contour [10] fails to segment the layers in the cornea due to very low signal to noise ratio of the cornea image.

Let $\Omega_{\alpha,\theta}(s)$, $(s \in [0,1], \alpha \in [0-\epsilon, 1+\epsilon], \theta \in [0, 360])$ be a parametric curve, represented using a spline, deformable model, or polynomial with s, the arclength as the parameter. The parameter ϵ is a small positive value allowing the algorithm to search for boundaries in the neighborhood surrounding $\alpha = 0$ and $\alpha = 1$.

In literature [7, 4] the curve $\Omega_{\alpha,\theta}(s) = \Omega(s)$ is modeled as an energy minimizing spline with total energy as:

$$E = \int_0^1 \left(\underbrace{\alpha(s)\Omega_s^2(s)}_{Elastic} + \underbrace{\beta(s)\Omega_{ss}^2(s)}_{Membrane} - \underbrace{\gamma(s)E_{ext}(\Omega(s))}_{External} \right) ds \tag{1}$$

where $\Omega_s(s)$ and $\Omega_{ss}(s)$ are the first and second derivatives of $v(s)$ with respect to the arclength s, and the parameters $\alpha(s), \beta(s)$ and $\gamma(s)$ are the penalties imposed on slope, curvature and the external force of the active contours, respectively. Typically, to allow convergence of the active contour to the image edges, the energy is defined to be a function of the image gradient (g),

$$E_{ext} = g^2(I) = (\delta G_\sigma * I)^2 \tag{2}$$

for some first derivative of Gaussian (δG_σ) with bandwidth σ, where $*$ is the convolution operator and $I \in [0,1]$ is the intensity map of the cornea image.

The goal is to obtain the corneal boundaries by minimizing equation (1). However, as one can see from Figure 2 the layers of the cornea are not distinct. Therefore, the gradient map alone is not able to attract the snake towards the layers of the cornea. Further, the layer boundaries of the cornea obey spatial statistics. Consequently, a model based

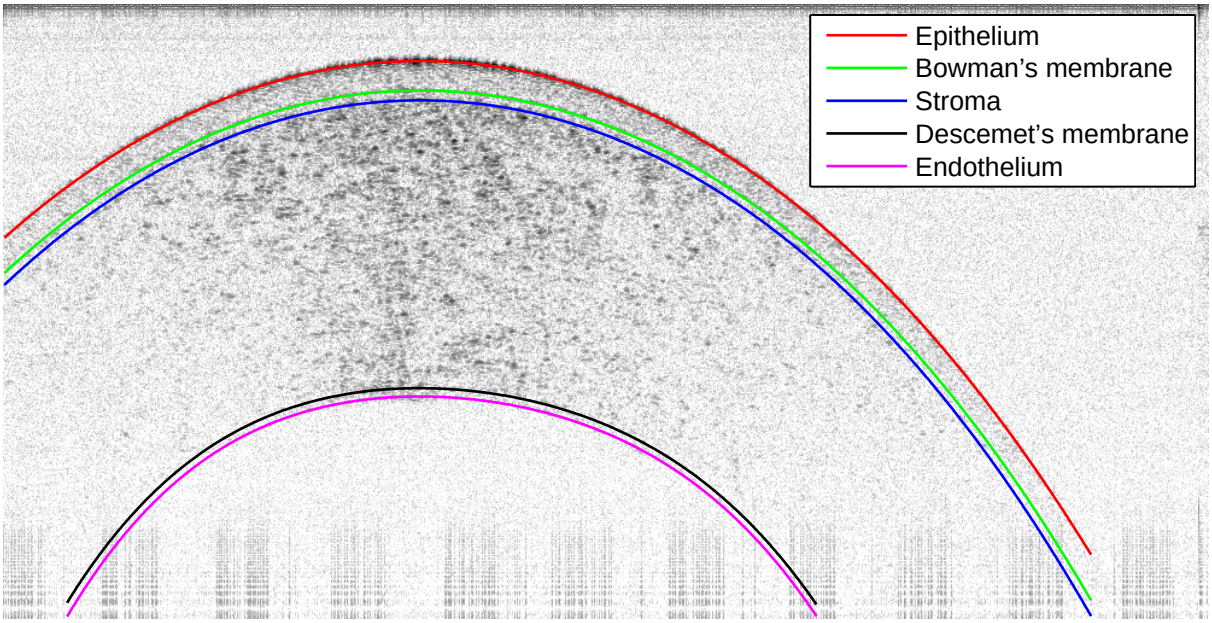

Figure 2. Cornea image with layers of interest. The epithelium and endothelium layers of the cornea are distinct while the other layers are obscured.

approach is suitable to segment the layers of the cornea. Unlike the active contour which uses a deformable model, the proposed method uses a prior model, $\Omega_{\alpha,\theta}(s)$ defined using parameters α and θ to represent the layer boundaries. The proposed method assumes there is a correspondence relationship between the layers and that each layer can be represented using a piecewise continuous non-deformable linear spline $\Omega_{\alpha,\theta}(s)$. The total cost associated with the spline is:

$$f(\alpha,\theta) = \oint_{\Omega_{(\alpha,\theta)}(s)} \big((1-I)^2 + g^2(I)\big)ds \qquad (3)$$

The goal is to obtain optimal value of α and θ corresponding to the maxima of $f(\alpha,\theta)$, Mathematically,

$$\left[\hat{\alpha},\hat{\theta}\right] = \arg\max_{\alpha,\theta}\left(f(\alpha,\theta)\right) \qquad (4)$$

An efficient approach to solve (4) is provided in Section 3.

3 Proposed Approach

This section describes how the proposed approach extracts the corneal layer boundaries. The proposed approach consists of three steps: 1) preprocessing 3.1, 2) obtaining correspondence model 3.2 and 3) locating the layers of the cornea 3.3.

3.1 Preprocessing

Preprocessing of the corneal image is performed to improve the ability of EIS to snap to the outer and innermost layer boundaries. This step improves the boundary contrast while reducing the contrast of other regions. Contrast-limited adaptive histogram equalization (CLAHE) is applied to obtain more consistent contrast throughout the entire image [17]. Morphological operators are then applied in the preprocessing phase of this algorithm to enhance low contrast edges on the epithelium and endothelium boundaries [15]. If these edges have higher contrast, IS will be better able to snap to the boundaries.

The boundaries are first enhanced using multiple structuring operators designed to enhance arch-like structures. The open operator is applied to a grey scale image for a horizontal line. The slope of the line is then increased and the open operator is applied again so that the previous horizontal response becomes connected to adjacent points on the curved boundary. The slope of the line is increased and the process is repeated, connecting all points on the curve. The slope is then decreased from the horizontal to connect points on the opposite side of the boundary layer, associated with negative slope. Finally, Gaussian blurring is applied to remove noisy edges and to create uniform regions that permit the enhanced intelligent scissors to more easily snap to the higher contrast boundaries.

3.2 Correspondence model

The proposed approach uses EIS [12], an user interactive segmentation method, on the preprocessed image to extract a rough outline of the epithelium and endothelium (Figure 2). Then, the proposed approach creates a correspondence model based on the initial user defined boundaries of the epithelium and endothelium layers; the two boundaries are related using medial axis transform.

Let $\Omega_{\alpha,\theta}(s)$, $(s \in [0,1]\alpha \in [0-\epsilon, 1+\epsilon], \theta \in [0, 360])$ be a parametric curve which can be represented using spline, deformable model, or polynomial with s, the arclength as the parameter.

The curve $\Omega_{\alpha,\theta}(s)$ can be defined from correspondences between the user segmented curves associated with the epithelium and endothelium boundaries. When $\alpha = 0$ and θ=0, $\Omega_{\alpha,\theta}(s)$ corresponds exactly to the user segmented epithelium boundary. Similarly, $\Omega_{\alpha=1,\theta=0}(s)$ corresponds to the user segmented endothelium boundary.

As α increases from $0-\epsilon$ to $1+\epsilon$, $\Omega_{\alpha,\theta}(s)$ transforms from the epithelium boundary to the endothelium boundary. This transformation relies on point to point correspondences between the two boundaries. For each point, $p_{\alpha=0,i}$, on the epithelium boundary, the corresponding point on the endothelium boundary, $p_{\alpha=1,i}$, is determined using medial axis transform theorem. This association can be represented by a vector v_i where $p_{\alpha,i} = p_{\alpha=0,i} + \alpha v_i$. When $\alpha = 1$, $p_{\alpha=1,i}$ corresponds to the curve $\Omega_{\alpha=1,\theta=0}(s)$.

The parameter θ determines the rotation associated with the curve. Points $p_{\alpha,i}$, are rotated about $p_{\alpha,i=0}$ for values of θ. The points on the epithelium and endothelium boundaries are defined for $\theta = 0$.

The function value $\Omega_{\alpha,\theta}(s)$, and the axes α, $theta$, and s are illustrated in Figure 3.

3.3 Extracting corneal layers

With curves $\Omega_{\alpha=0,\theta=0}(s)$ and $\Omega_{\alpha=1,\theta=0}(s)$ defined from the user segmentation results, optimization techniques are applied to search for feasible values of α and θ that produce local maxima of equation (3). From the prior statics obtained from segmenting several hundred cornea images using the proposed algorithm, all five layers obey the same correspondence relationship as the correspondence relationship between epithelium and endothelium. Therefore, all five layers have the same orientation; the orientation is fixed at $\theta = 0$. So, (3) can be written as

$$f(\alpha) = \oint_{\Omega_{(\alpha,\theta)}(s)} \big((1-I)^2 + g^2(I)\big)ds \qquad (5)$$

The goal is to obtain optimal value of α and θ corresponding to the maxima of $f(\alpha, \theta)$, Mathematically, from the prior

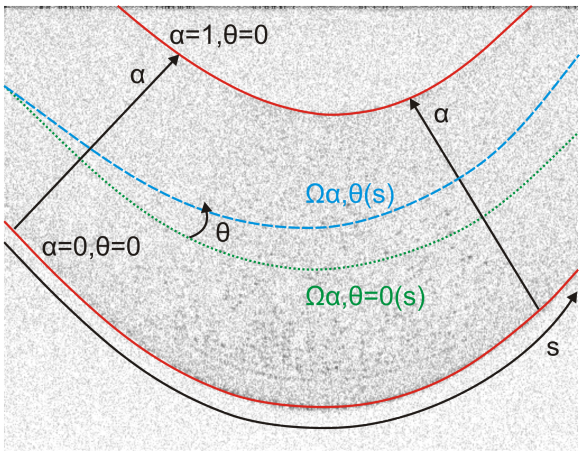

Figure 3. The function value $\Omega_{\alpha,\theta}(s)$ is shown in blue, and the axes α, $theta$, and s are shown in black. The upper and lower boundaries, in red, define the shape of the function $\Omega_{\alpha,\theta}(s)$.

knowledge, the five peaks corresponding to the five layers of the cornea are associated with the minima of $f(\alpha)$. However, the direct extraction of these peaks is difficult due to the non-linear and noisy nature of the function $f(\alpha)$. Therefore, the proposed algorithm incorporates prior knowledge associated with the spatial location of the layers of the cornea into $f(\alpha)$.

Based on a large sample set of 800 corneal images, a probability density function in the form of a Gaussian mixture model is created for the five values of α as follows:

$$\psi(\alpha) = \sum_{i=1}^{5} (\aleph(\mu_i, \sigma_i)) \qquad (6)$$

Where μ_i and σ_i are the mean and standard deviation of the layers. Proposed approach obtains a bilateral function $\Upsilon(\alpha)$ by:

$$\Upsilon(\alpha) = f(\alpha) * \psi(\alpha). \qquad (7)$$

The five values of α corresponding to five significant peaks of $\Upsilon(\alpha)$ are obtained and assigned to the five corresponding corneal layer boundaries.

4 Test Results and Discussions

This section demonstrates the performance of the proposed method compared to EIS and IS over a set of representative corneal images. Other segmentation methods were also tested, but, since they were dependent on the image gradient, failed completely for the corneal images.

4.1 Methods Compared

In this section, the performance of the proposed method is compared to enhanced intelligent scissors (EIS) and to intelligent scissors (IS); EIS and IS are both user interactive segmentation methods. The proposed approach requires user input when extracting the upper and lower layers of the cornea. Using the user inputs to define the shape of the cornea, the method accurately extracts all five layer boundaries. The performance of the level set (LS) [10] and gradient vector flow based snake (GVFS) [16] was tested on a subset of cornea images. Since, the images are noisy and lack significant gradient information, LS and GVFS did not produce any meaningful results on test data sets. Therefore, LS and GVFS were excluded from further consideration.

4.2 Data Sets and Experimental Set up

The proposed algorithm was executed on corneal tomograms acquired by Department of Physics and Astronomy at the University of Waterloo. The images, containing 512 by 512 pixels, were obtained from three test subjects using a variety of OCT imaging techniques. One technique produced a high contrast edge of the epithelium layer, located at cornea to air interface. The focus of the tomogram was centered at this point, which produced a high contrast epithelium layer, but a low contrast endothelium layer. A second technique inverted the corneal image by focusing on the endothelium layer. Since the refraction index differed for each layer boundary, the second method produced medium contrast for both the endothelium and epithelium layers. The other, less preferable, imaging techniques produced artifacts within the corneal image; they created dark artifacts through the apex of the cornea or vertical white bands distributed over the entire cornea. These artifacts are the result of imperfect hardware configurations and cause the visibility of the corneal image to become obstructed. The algorithms are evaluated for images representing each type of technique.

In this section, the proposed method, EIS, and IS are evaluated using five representative samples from the data set that illustrate the various imaging techniques executed during the data collection process. The segmentation results were obtained using a dual core 2.5 GHz computer with 2 GB of RAM. The algorithms considered for evaluation are implemented in Matlab R2008b.

4.3 Segmentation Results

The segmentation result of proposed method, EIS, and IS across five cornea images are shown in Figure 4. Each corneal image contains five layer boundaries that must be segmented so that the thickness of each layer can be measured. In all test images, the proposed approach successfully extracts the layers of the cornea. The segmentation results for EIS and IS primarily depend upon the interaction capability of the user; better results are produced as the user manually specifies more points. Both EIS and IS require about 10 to 15 minutes for the manual user input for each image to produce the level of accuracy shown in Figure 4.

To evaluate the accuracy of the algorithms, the ground truth for each image is specified by manually selecting points on each layer boundary. This process requires about 15 minutes of manual user input to specify over 100 points for each image. The algorithms are evaluated by how close the segmented boundaries are to the ground truth. For each point along the ground truth boundary, the shortest distance between the ground truth and the segmentation result is calculated. The average distance and standard deviation is computed for each layer. The results are summarized in Figure 5.

On average, the proposed algorithm successfully locates the layer boundary within 1.5 pixels of the manually specified ground truth. This algorithm typically requires the user to specify only 4 points. In addition, when acquiring statistics, about 800 images were segmented using less than 20 seconds worth of manual user input per image. The amount of user interaction required to obtain the level of accuracy permits large numbers of corneal measurements to be obtained in sufficiently less time than is required for manual segmentation.

The use of the EIS to outline the cornea and model of the various layers allows the proposed algorithm to be capable of greater accuracy than fully-automated algorithms by accommodating significant amounts of noise. For the tests sets with the greatest number of artifacts, image #1 and image #3, the maximum deviation of the generated boundaries is within 4 pixels of the manually specified boundaries. In addition, the algorithm also performs well for low contrast regions, such as image #5.

When compared to the other methods, the proposed algorithm produces boundaries that are closer to the ground truth than those produced by EIS or IS. The standard deviation for the proposed algorithm is also less, indicating a more consistent boundary over the entire image. Although all methods perform well for the higher contrast layer boundaries (the epithelium and endothelium), the proposed algorithm performs significantly better than EIS and IS for the middle layers, as shown in Figure 5. The proposed algorithm provides a smoother curve that is less prone to noise and artifacts present in many of the images, as shown in Figure 4. The proposed method also requires significantly less user interaction. As a consequence, more accurate boundaries can be measured from minimal user input.

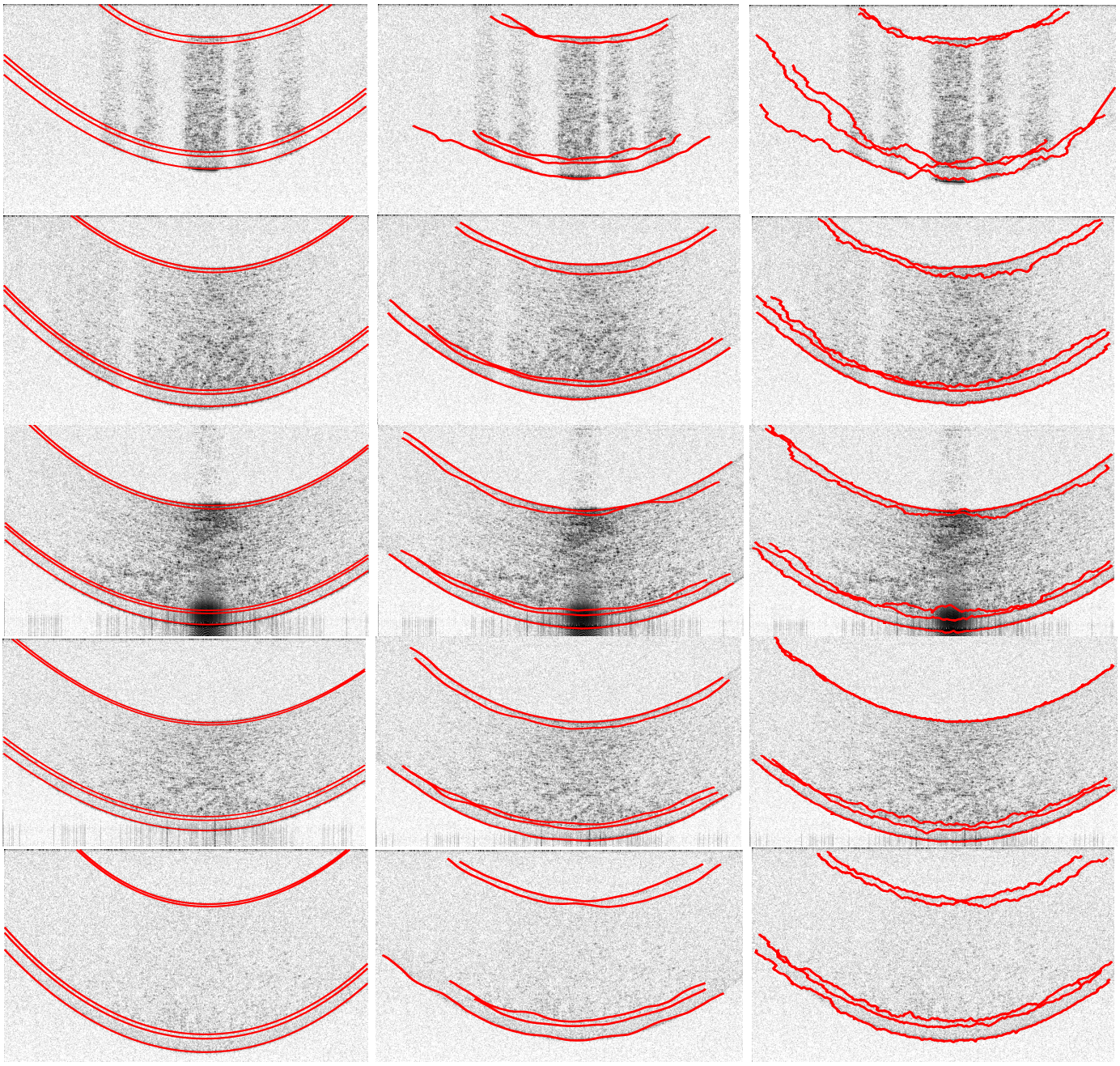

Proposed method EIS [12] IS [5]

Figure 4. Demonstration of the performance of proposed method compared to other published methods across five cornea images. Column 1: results obtained using proposed approach. Column 2-3: results obtained using enhanced intelligent scissor (EIS) and intelligent scissor (IS). From top to bottom the images contain the following artifacts: multiple white bands distributed over the entire image, a single white band on the left side of the image, a dark artifact located at the apex of the epithelium layer, typical image with good contrast, and typical image with very low contrast.

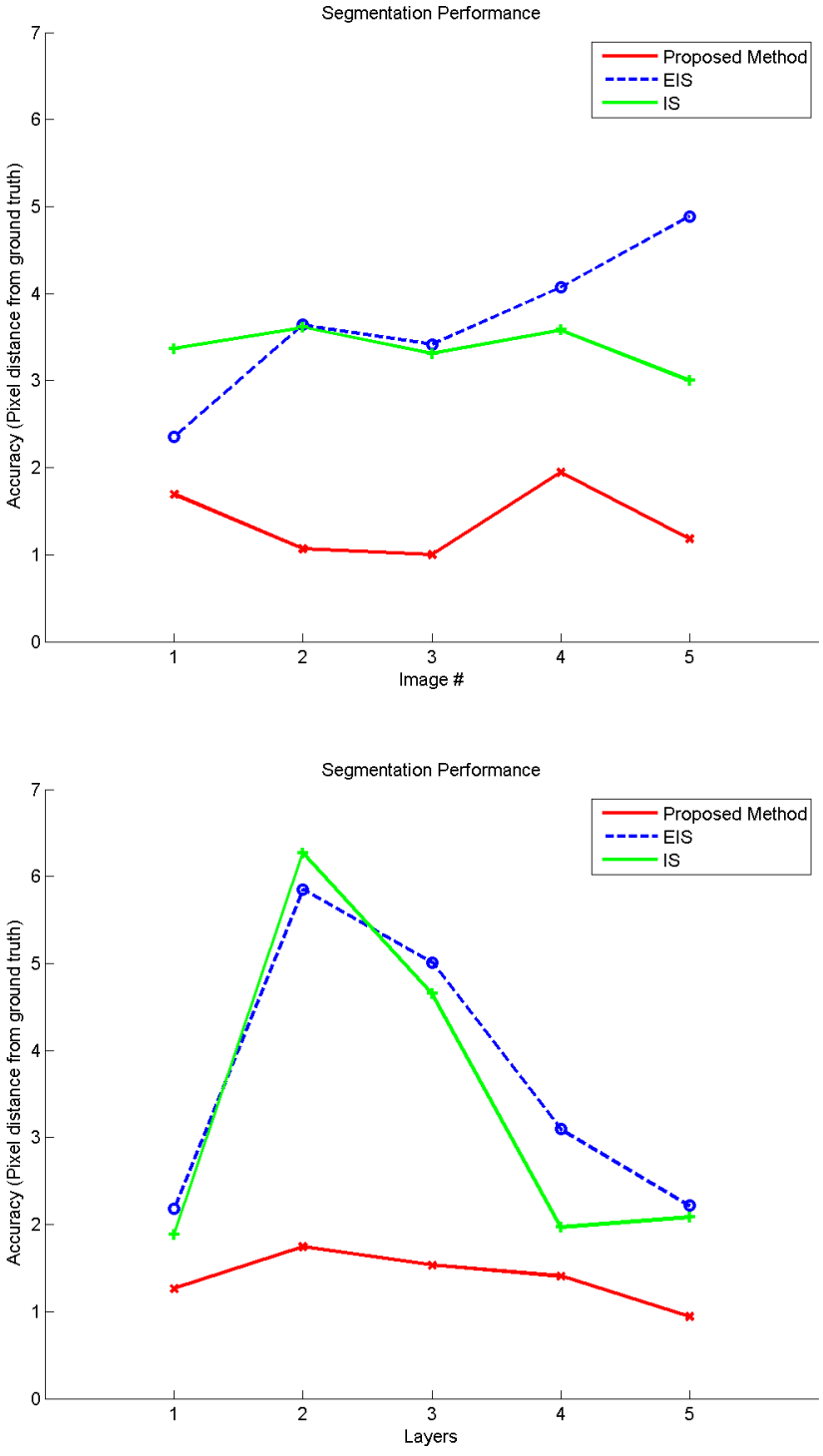

Figure 5. Performance index of proposed approach compared to enhanced intelligent scissor (EIS) and intelligent scissor (IS). The layers 1-5 corresponds to epithelium, Bowman's membrane, stroma, Descemet's membrane and the endothelium layers of the cornea respectively. The proposed algorithm performs as well or better than EIS and IS for all layers and images in the test set. Level set (LS) and Gradient vector flow based snake (GVFS) are not shown because their errors exceeded 200 pixels.

5 Conclusion and Future work

This paper establishes and evaluates a novel algorithm for segmentation of the layers of the cornea. The algorithm accurately determines layer boundaries of the cornea images for a variety of corneal imaging techniques. For images with large numbers of artifacts, on average, the algorithm is able to determine the boundaries to be within 1.5 pixels of the actual boundaries. The proposed algorithm is able to produce these results with significantly less user input than fully manual segmentation. The proposed algorithm is capable of segmenting images with large artifacts or speckle noise. The use of a corneal model and minimal user input allows the cornea to be segmented without explicitly denoising the image. Consequently, the algorithm is robust to low signal to noise ratios. Future work will attempt to fully automate the segmentation process and will consider additional parameters, such as scale and rotation, to improve the local optimization process when fitting the spline boundaries to the image data.

6 Acknowledgement

This research has been sponsored by the Natural Sciences and Engineering Research Council (NSERC) of Canada through individual Discovery Grants as well as GEOIDE (GEOmatics for Informed Decisions) which is a Network of Centres of Excellence under NSERC.

References

[1] L. Alvord, W. Hall, L. Keyes, C. Morgan, and L. C. Winterton. Corneal oxygen distribution with contact lens wear. *Cornea*, 26(6):654–664, July 2007.

[2] A. A. Amini, T. E. Weymouth, and R. C. Jain. Using dynamic programming for solving variational problems in vision. *IEEE Transaction on Pattern Analysis and Machine Intelligence*, 12(9):855–867, 1990.

[3] T. Chan and L. Vese. Active contours without edges. *IEEE Transaction on Image Processing*, 10(2):266–277, 2001.

[4] L. Cohen. On active contour models and balloons. *Computer Vision Graphics and Image Understanding*, 53(2):211–218, March 1991.

[5] N. M. Eric and A. B. William. Intelligent scissors for image composition. In *SIGGRAPH '95: Proceedings of the 22nd annual conference on Computer graphics and interactive techniques*, pages 191–198, New York, NY, USA, 1995. ACM.

[6] E. Hancock and J. Kittler. Edge-labeling using dictionary-based relaxation. *IEEE Transaction on Pattern Analysis and Machine Intelligence*, 12(2):165–181, February 1990.

[7] M. Kass, A. Witkin, and D. Terzopoulos. Snakes: Active contour models. *International Journal of Computer Vision*, 1(4):321–331, 1988.

[8] R. Khurana, Y. Li, M. Tang, M. Lai, and M. D. Huang. High-speed optical coherence tomography of corneal opacities ophthalmology. *Ophthalmology*, 114(7):1278–1285, July 2007.

[9] M. Madigan, P. Penfold, and B. Holden. Ultrastructural features of contact lens- induced deep corneal diseases. *Cornea*, 9:144–151, 1990.

[10] R. Malladi, J. A. Sethian, and B. C. Vemuri. Shape modeling with front propagation: A level set approach. *IEEE Transaction on Pattern Analysis and Machine Intelligence*, 17(2):158–175, 1995.

[11] D. Minsky and M. Feigin. Optimal boundary detection on grey-tone image. *Pattern Recognition*, 30(6):971–998, June 1997.

[12] A. Mishra, A. Wong, W. Zhang, D. Clausi, and P. Fieguth. Improved interactive medical image segmentation using enhanced intelligent scissors (eis). In *Annual International Conference of the IEEE Engineering in Medicine and Biology Society*, August 2008.

[13] E. Pisano. Contrast limited adaptive histogram equalization image processing to improve the detection of simulated spiculations in dense mammograms. 11.4:193, 1998.

[14] P. Puvanathasan and B. K. Interval type-ii fuzzy anisotropic diffusion algorithm for speckle noise reduction in optical coherence tomography images. *Opt. Express*, 17:733–746, 2009.

[15] R. Stevenson and G. Arce. Morphological filters: Statistical and further syntactic properties. 34(11):1292–1305, November 1987.

[16] C. Xu and J. Prince. Snakes, shapes, and gradient vector flow. *IEEE Transaction on Image Processing*, 7(3):359–369, 1998.

[17] K. Zuiderveld. Contrast limited adaptive histogram equalization. pages 474–485, 1994.